Classical and weak localization processes in a tunable ballistic-electron cavity

R. P. Taylor, R. Newbury, and R. B. Dunford
School of Physics, University of New South Wales, Sydney 2052, Australia

P. T. Coleridge, A. S. Sachrajda, and J. A. Adams
Institute for Microstructural Sciences, National Research Council, Ottawa, Canada K1A 0R6
(Received 16 August 1994)

The appeal of the lateral surface gate technique lies in the ability to tune the device through application of variable gate bias. We apply positive bias to a 250-nm-wide continuous gate, or stripe, defined above the two-dimensional electron gas of an $Al_xGa_{1-x}As/GaAs$ heterostructure. Following pulsed light emitting diode illumination, inhomogeneities in the region shielded by the stripe can be annealed by tuning the positive bias. We employ this technique to introduce trajectory scrambling events into a ballistic-electron cavity. Through a systematic study of the low-field magnetoresistance of the cavity as a function of positive stripe bias (tuning the inhomogeneities) and temperature (control of electron phase coherence), we examine the interplay between geometry-induced weak localization and classical transport phenomena. In contrast to other recent observations of weak localization in the ballistic regime, our cavity is relatively large (1.8×30 μm^2) and the trajectory loops are defined, not by the confining walls of the cavity, but by the profile of the exit port.

I. INTRODUCTION

Advances in precision electron-beam lithography (EBL) have made it possible to fabricate devices in which electrons travel ballistically and maintain their phase coherence over distances larger than the device size when cooled to liquid-helium temperatures.[1] These devices exhibit a range of magnetotransport effects, induced predominantly by the artificially imposed geometry rather than intrinsic, material-related scattering processes. Recent interest has focused on the quantum-mechanical limit of classically chaotic systems–quantum chaos.[2,3] A variety of enclosed geometries, or cavities, can be defined using electrostatic gates constructed above high electron mobility systems, such as the two-dimensional electron gas (2DEG) formed at the $Al_xGa_{1-x}As/GaAs$ interface. In the traditional mode of operation, a negative gate bias is applied to establish partial or complete electron depletion under the gate pattern, and patterns have been designed where the cavity evolves between two distinct geometries as a function of the negative gate bias.[4] In this paper we demonstrate a different approach to the use of surface gates to induce a controlled transition in the cavity. A positive bias is applied to a 250-nm-wide continuous gate, or stripe, defined on the surface of an $Al_xGa_{1-x}As/GaAs$ heterostructure. Following pulsed illumination with a light-emitting diode (LED), the region shielded by the gate is highly inhomogeneous and this can be annealed in a controlled, reversible fashion by tuning the positive gate bias. Such a stripe can be used to introduce scrambling events into a ballistic cavity and to perturb classical and phase-coherent magnetotransport processes. We employ the technique to investigate geometry-induced weak localization, a phenomenon which is generating considerable experimental[3,5,6] and theoretical[2] interest. In contrast to recent observations in submicrometer cavities, we adopt a much more open geometry (1.8×30 μm^2) which supports only a selected number of phase-coherent trajectory loops, and this eliminates magnetoconductance fluctuations.[2] This simplifies the weak-localization analysis since uncertainties can arise from separating the weak localization from the superimposed aperiodic fluctuations. We investigate the effect of the stripe gating action on the interplay of classical collimation and weak-localization processes in the ballistic cavity.

II. DEVICE CHARACTERISTICS

The device, which consists of two split gates in series and one continuous stripe gate bisecting the region between the split gates, is shown in the scanning electron micrograph inset to Fig. 1. The five gates (each of width 250 nm) were defined by EBL and deposited on the surface of a 30-μm-wide Hall bar using the lift-off process.[4] Figure 1 shows typical gate characteristics taken at 1.5 K for the component gates, with the split gate revealing conductance plateaus associated with the formation of a quantum point contact (QPC). The two QPC's serve as entrance and exit ports to a confined cavity with lithographic dimensions $W=30$ μm and $L=1.8$ μm. To check for reproducibility of the effects reported, the device has been thermally cycled five times and, after illumination (see below), the electron mobility and electron density were in the ranges $\mu=(25-45)$ $m^2V^{-1}s^{-1}$ and $n_s=(1.9-3.6)\times10^{15}$ m^{-2}, respectively, corresponding to mean free paths $L_t=(2-4.5)$ μm. The QPC's therefore inject and collect a collimated beam of ballistic electrons which passes under the stripe traversing the cavity.

Using a red LED mounted on the device header, the illumination process consists of a sequence of 100-ms pulses at 4 K, with all gates grounded to the 2DEG. In

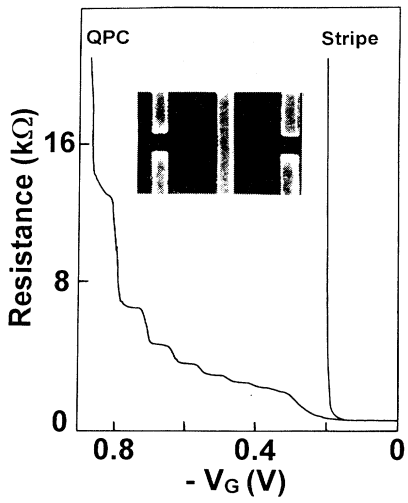

FIG. 1. The inset is a scanning electron micrograph of the five-gate device. Each gate is 250 nm wide. The main traces show typical characteristics for the component gates as a function of negative bias. $T=1.7$ K.

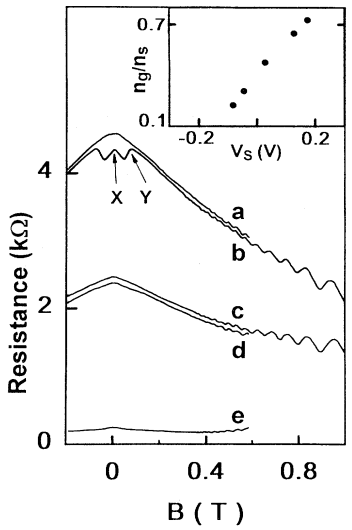

FIG. 2. Magnetoresistance traces with +0.5 V applied to the stripe: (*a*) the arithmetic addition of the resistances R(QPC1)+R(QPC2)−R(Bulk), (*b*) the device resistance, (*c*) R(QPC1), (*d*) R(QPC2), and (*e*) R(Bulk). See text for details of features X and Y. The inset shows the ratio n_g/n_s as a function of stripe bias V_s. $T=1.7$ K and $n_s=3.6\times10^{15}$ m^{-2}.

the exposed (i.e., ungated) regions, n_s increased due to the well-known persistent photoconductivity effect,[7] and the sequence is continued until n_s saturates. Typically, n_s increased by 40% during the complete illumination process. In contrast, the regions under the gate are partially shielded from the light. The gates consist of a 10-nm Ti metallization (chosen for its reproducible Schottky barrier and superior adhesion properties) capped by a 40-nm layer of Pt. Based on our previous low-temperature optical transparency tests of thin (8–50 nm) gates,[8] we estimate the skin depth (δ) of the gates to be less than 20 nm at the LED wavelength, and therefore that less than 10% of the light will penetrate the gate metallization. Notwithstanding this, diffraction processes will result in a partial, nonuniform exposure of the shielded region. We believe that the region under the stripe is described by an electron density n_g smaller than the bulk, and which has a nonuniform spatial distribution. We also note that electron-beam damage during fabrication will be strongest in the gate regions, further adding to the inhomogeneous character of the stripe.

Four terminal measurements were made across the gated region of the Hall bar using low-frequency ac measuring techniques, with typical currents of 10 nA at dilution refrigerator temperatures. Low-field Shubnikov–de Haas oscillations indicate an increased homogeneity in the Hall bar's electron density as positive bias is applied to the gates. Furthermore, the accuracy of conductance plateaus of the QPC's can be improved by positively biasing the neighboring gates. Both results are consistent with a positive bias removing the effect of the presence of a gate. At magnetic fields sufficiently high for edge-state transport, the stripe reflects selected edge states, allowing a calculation of n_g as a function of stripe bias V_s.[1] The ratio n_g/n_s is found to be as low as 40% for zero bias, and this increases smoothly as a function of positive bias.[9] A typical stripe bias characteristic is shown in the inset of Fig. 2. Provided biases of 0.7 V are not exceeded, the gating action is found to be reversible. Higher biases match the Schottky barrier height (0.77–1 eV), and the resulting gate leakage current causes a redistribution of charge in the intermediate material layers, altering the gating characteristic. Thermal cycling and/or reillumination similarly results in a modified characteristic.

III. LOW-FIELD CLASSICAL MAGNETORESISTANCE

Figure 2 shows the magnetoresistance of the device taken at $T=1.2$ K following pulsed illumination ($n_s=3.6\times10^{15}$ m^{-2}). The gating action, characterized by the same cooldown, is shown in the inset, and from this we find that the presence of a particular gate can be minimized by applying a +0.5-V bias. First consider the behavior of the individual components of the device. Each QPC separately shows the characteristic negative magnetoresistance associated with magnetic depopulation of the Landau levels in the bulk 2DEG (Fig. 2, traces *c* and *d*). Within the Landauer-Buttiker formalism,[10] the magnetoresistance is determined by the number of occupied subbands in the QPC ($N_{\rm qpc}$) and in the bulk ($N_{\rm bulk}$).[1,11] For low magnetic fields, $N_{\rm qpc}$ is essentially independent of field and $N_{\rm bulk}$ is the number of Landau levels. The four-terminal resistance of a QPC, $(h/2e^2)(1/N_{\rm qpc}-1/N_{\rm bulk})$, then has a negative slope equal to the Hall slope, as observed. For the stripe there is a different behavior. When the cyclotron diameter $2R_B$ is less than the stripe width ($B>0.25$ T) the number of occupied Landau levels in the stripe region ($N_{\rm stripe}$) will, depending on the gate bias, be less than $N_{\rm bulk}$. The appropriate term $(h/2e^2)(1/N_{\rm stripe}-1/N_{\rm bulk})$ then results

in a positive magnetoresistance. At lower fields, when the cyclotron diameter is larger than the stripe width, the magnetoresistance of the stripe is expected to be effectively constant, followed by the transition to the higher-field positive slope.[12,13] In practice, due to the stripe's narrow width, the positive magnetoresistance is found to be partially suppressed by transmission of electrons across the stripe and, at the +0.5-V bias, can be ignored for the field range considered here.[12]

In Fig. 2, trace *b* is the magnetoresistance of the device with both QPC's formed and the stripe biased at +0.5 V. The high-field magnetoresistance (above about 0.1 T, marked *Y*) closely matches trace *a*, the arithmetic sum of the effects of the separate QPC's (with the appropriate correction for double counting of the bulk contribution). At fields below *Y*, there is a dip in the resistance of trace *b* and a small central peak (labeled *X*). The peak will be discussed below. The dip is attributed to a collimated beam of ballistic electrons propagating through both QPC's,[1,11,14] giving the standard nonadditive result.[15] Increasing the field deflects the beam, reducing the number of directly transmitted electrons until, when R_B matches L, all trajectories are directed into the upper (or lower, depending on current and field direction) region of the cavity where the electrons' phase is randomized.[11,16] The full angular spread of the ballistic beam, 2α, measured from the ratio L/R_B (Ref. 1) at the field B_c at which the resistance changes from nonadditive to additive (i.e., at feature *Y*) is 98°. In contrast, the angle calculated assuming classical collimation factors for the QPC is 74°.[1,11] Previous QPC studies, using a similar cavity but without a central stripe, also gave an angle larger than that expected for a classical injector, and the deviation was attributed to electron-diffraction effects (the QPC width and Fermi wavelength are of a similar magnitude).[16] In the case of our device, inhomogeneities associated with the stripe will further add to the broadening of the beam.

Figure 3 shows the same magnetoresistance features as a function of stripe bias, measured on the same device following thermal cycling and reillumination. The change in device resistance is due to a change in QPC bias settings: in Fig. 3, the QPCs are tuned to each transmit four subbands, whilst for Fig. 2 the bias was less negative. Note that feature *Y* has moved to lower fields. This is partly the result of a decrease in n_s (2×10^{15} m^{-2}) and also the higher QPC bias producing a more collimated beam ($2\alpha=65°$).[1,11] As the positive stripe bias is reduced from 0.5 to 0.3 V, the ratio n_g/n_s decreases and the cavity becomes less homogeneous, so scrambling the collimated beam. This reduction in the number of ballistic (directly transmitted) electrons is evident in the weakening of the resistance dip. In the negative bias regime, as n_g/n_s decreases below 50% and the depletion region starts to form a well-defined barrier, a broad central peak emerges accompanied by a large rise in device resistance (Fig. 3, trace *a*). This is attributed to ballistic reflection of electrons by the barrier back through the entrance QPC. The effect of the stripe on one or both QPCs is, as a result, highly nonadditive: R(QPC1+Barrier) $>R$(QPC2)+R(Barrier). For example, the extra resistance of the stripe by itself is approximately 50Ω, but with the QPC's formed it adds a resistance of 3 kΩ. Application of a magnetic field deflects the backscattered electrons away from the entrance QPC and suppresses field at which R_B matches the spacing between the strip and QPC (0.65 μm, allowing for a lateral depletion of 50 nm). This calculation is in agreement with the measured width of Fig. 3, trace *a*. In this negative bias regime, the well-defined barrier suppresses the ballistic propagation across the cavity and encourages equilibration of electrons on either side of the barrier. This gives the observed result, expressed by the approximate equality: R(QPC1+ Barrier) + R(QPC2+Barrier) ≈R(QPC1+ QPC2+Barrier). This equation is approximate because, as has already been noted, the barrier alone adds 50Ω only whilst barrier plus QPCs adds 3 kΩ; the important point here is the resistance added by the interaction of barrier and QPCs. Suppression of ballistic propagation is made complete by magnetic fields strong enough that the electrons are confined to skipping orbits along the edges of the gates defining the QPCs.

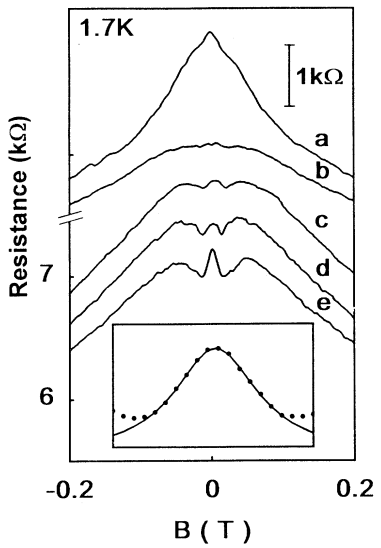

FIG. 3. The effect of stripe bias V_s on the device magnetoresistance. The traces have been vertically offset for clarity. The V_s and zero-field resistances are (*a*) −0.19 V and 9.68 kΩ, (*b*) −0.04 V and 7.19 kΩ, (*c*) +0.13 V and 7.12 kΩ, (*d*) +0.18 V and 7.15 kΩ and (*e*) +0.5 V and 7.26 kΩ. The bar marker refers to traces *a* and *b* only: the vertical scale of these traces is half that for the others. $T=1.7$ K and $n_s=2\times10^{15}$ m^{-2}. The inset shows a Lorentzian fit (solid line) to the data (dots) of trace *e*.

IV. GEOMETRY-INDUCED WEAK LOCALIZATION

We now return to peak *X*. Preliminary measurements[12] tentatively attribute this feature to a change in current distribution that accompanies the transition from low field ($\mu B \ll 1$, where the distribution is determined by the path of maximum conductivity) to high field [$\mu B \gg 1$, when the Hall term (σ_{xy}) dominates and the

distribution is determined by local Hall resistance and hence electron-density variations across the gated region] behavior. However, the peak width given by $\mu B = 1$ is 0.04 T, which is more than twice that observed. Furthermore, the peak's temperature dependence would be expected to follow that of peak Y since both would be determined by μ. Figure 4(a) demonstrates that peak X has a much sharper temperature dependence by plotting the normalized height of peak X (the ratio r_N of the heights of peak X and Y, both measured relative to the resistance minimum at around 0.01 T) as a function of temperature. The classical feature Y shows only a small change in resistance (30 Ω over the temperature range shown), indicating a temperature saturation of μ. The temperature dependence of the ratio therefore essentially reflects that of peak X and can be fitted to the expression $\exp(-L_D/L_\phi)$, if we assume $L_\phi \alpha T^{-p}$ [within the experimental uncertainty the data are consistent with both $p = 2/3$, shown in Fig. 4(a), and $p = 1$ (Ref. 17)]. This form suggests a quantum-mechanical origin, with the process magnitude governed by an electron phase-coherence length L_ϕ (Ref. 17) and a characteristic electron traversal length L_D. We can dismiss injection effects relating to standing-wave modes supported by the cavity, since for these to be resolved temperatures below 50 mK would be required to reduce thermal broadening. Because the dimensions of the cavity are significantly larger than the Fermi wavelength ($\lambda_F = 55$ nm), a semiclassical picture is appropriate: the effect is reminiscent of weak localization (WL).[18] See, for example, Fig. 4(b), showing the low-field magnetoresistance at $T = 50$ mK. Since the potential profiles of the QPC's are expected to be rounded,[1] the device geometry does indeed define time-reversed pairs of trajectories, each starting and ending in the same subband of the entrance QPC. The associated coherent backscattering of the electron waves increases the zero-field resistance above its classical value by an amount determined by the electron phase coherence and hence temperature. The inset to Fig. 4(a) shows a schematic representation of the simplest trajectory, although more complex reentrant loops do exist.[19] Constructive interference is lost when the order of one flux quantum ($\phi_0 = h/e$, where h is Planck's constant and e is the electronic charge) threads the enclosed area A of a typical loop. For the triangular loop, $B_\phi = \phi_0/2A$ (the factor of 2 arises because, in effect, the loop is traversed twice during the WL process[18]) predicts an approximate peak width of 0.01 T, close to that observed. We note that negative magnetoresistance features were also evident in the data from other ballistic cavities incorporating two QPC's positioned opposite each other, although the origin of these features was not addressed.[20,21]

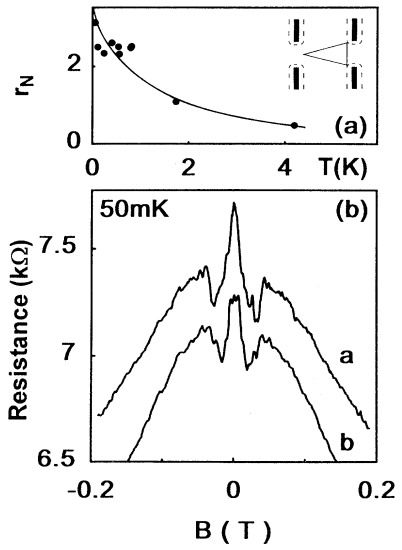

FIG. 4. (a) The normalized peak amplitude r_N as a function of temperature with a fit using $p = \frac{2}{3}$ (see text for details). $V_s = +0.7$ V. The inset shows a schematic representation of a simple trajectory loop created by the rounded profiles of the entrance and exit ports. (b) Magnetoresistance of the device taken at $T = 50$ mK for stripe biases of (*a*) +0.7 V and (*b*) +0 V. Trace *b* is offset by 250 Ω for clarity. $n_s = 2 \times 10^{15}$ m^{-2}.

The theory of WL in ballistic devices is highly topical.[2] The predicted correction to the classical resistance can be large[2] and for our 50-mK data, Fig. 4(b), the correction is 8%. In the limit $B_\phi \ll B_c$, the classical bending of trajectories can be ignored for fields smaller than B_ϕ. The WL magnetoresistance is then determined only by the phase difference which appears between the time-reversed paths, and its exact line shape will be sensitive to the distribution of loop areas supported by the geometry. Semiclassical analysis highlights a fascinating feature of ballistic WL, not apparent for the analogous effect in disordered systems:[18] the WL magnetoresistance line shape will distinguish between chaotic and nonchaotic dynamics.[2] For our cavity $B_\phi/B_c = 0.3$, and the inset to Fig. 3 shows a Lorentzian fit to the low-field magnetoresistance of Fig. 3(e). The half-width of the fit is 0.01 T, identical to the width calculated assuming the characteristic area to be that of the simple triangular loop. The Lorentzian form has also recently been applied to the magnetoresistance of a chaotic geometry.[5,2] The unique quality of our device lies in the aspect ratio of the cavity. L is sufficiently small to allow the WL trajectory loops to remain phase coherent, but W is so large that more complex loops, confined by the cavity's width, do not contribute because of their length. For this reason, aperiodic fluctuations, which are seen in the magnetoresistance of more confined geometries,[3,5,6,22] and which arise from quantum interference between paths which do not return to their originating QPC subband, are not generated by our cavity. Since fluctuations are not superimposed on the WL magnetoresistance, our device geometry is highly suited to studies of the WL phenomenon. We note also that, for studies of WL in submicron stadia,[3,5,6] the entrance and exit ports are deliberately offset to eliminate direct paths which do not interact with the edges of the cavity. In contrast, for our geometry the ports should be aligned in order to most effectively define the WL loops; the effect was not observed in similar cavities where the ports are offset by 190 nm.[16]

Finally, we consider the effect of the stripe on the WL feature. When the cavity is clean (at the lowest temperatures, to remove phase randomization processes, and highest positive stripe bias, to remove inhomogeneities)

the WL process is strongest. The WL loops are scrambled by introducing the inhomogeneous region under the stripe, and the peak therefore decreases as the positive bias is reduced. Peak X is more sensitive than peak Y to the introduction of the inhomogeneous region under the stripe (see Fig. 3) because this region is traversed four times during the WL process, whereas this traversal occurs only once for the classical collimation effect. We speculate that the variation in the size of peak X between different cooldowns reflects the sensitivity of the WL process to the precise potential profiles of the QPCs and under the stripe[23] [note that the larger peak of Fig. 3(trace *e*) compared to Fig. 2(trace *b*) is also partially attributable to the narrower beam increasing the number of electrons directed at the exit QPC, allowing a larger fraction of electrons to contribute to the WL process]. WL is completely suppressed at negative stripe biases when the stripe barrier prevents the majority of electrons from traversing the cavity.

V. CONCLUSIONS

Following pulsed illumination with a LED, a 250-nm stripe has been used to tune the homogeneity of a 2DEG cavity through application of positive gate bias. We have compared the effect of introducing scrambling events on the magnetoresistance features generated by the cavity. We have distinguished a quantum process from the classical ballistic processes through its increased sensitivity to both temperature and inhomogeneities introduced under the stripe, and have identified the quantum effect in this device as geometry-induced weak localization. Due to the aspect ratio of the cavity, the magnetoresistance does not exhibit the aperiodic fluctuations observed in more confined cavities such as the stadium geometry. Future experiments will investigate the precise dependence of the WL process on temperature and beam spread.

ACKNOWLEDGMENT

We thank J. M. Cadogan for expert assistance with the magnetoresistance analysis.

[1]See, for example, review articles by C. W. J. Beenakker and H. van Houten, in *Solid State Physics,* edited by H. Ehreneich and D. Turnbull (Academic, New York, 1991), Vol. 44, p. 1; S. E. Ulloa, A. Mackinnon, E. Castano, and G. Kirczenow, in *From Ballistic Transport to Localization,* edited by P. T. Landsberg, Handbook of Semiconductors Vol. 1 (North-Holland, Amsterdam, 1992).

[2]R. A. Jalabert, H. U. Baranger, and A. D. Stone, Phys. Rev. Lett. **65**, 2442 (1990); H. U. Baranger, R. A. Jalabert, and A. D. Stone, in *Transport Phenomena in Mesoscopic Systems,* edited by H. Fukuyama and T. Ando (Springer, New York, 1992); Chaos **3**, 665 (1993).

[3]C. M. Marcus, A. J. Rimberg, R. M. Westervelt, P. F. Hopkins, and A. C. Gossard, Phys. Rev. Lett. **69**, 506 (1992); C. M. Marcus, R. M. Westervelt, P. F. Hopkins and A. C. Gossard, Phys. Rev. B **48**, 2460 (1993).

[4]R. P. Taylor, J. Nanotech. (to be published).

[5]M. J. Berry, J. A. Katine, C. M. Marcus, R. M. Westervelt, and A. C. Gossard, Surf. Sci. **305**, 495 (1994).

[6]M. W. Keller, O. Millo, A. Mittal, D. E. Prober, and R. N. Sacks, Surf. Sci. **305**, 501 (1994).

[7]J. Klem, W. T. Masselink, D. Arnold, R. Fischer, T. J. Drumond, K. Morkoc, K. Lee, and M. S. Shur, J. Appl. Phys. **54**, 5214 (1983); D. K. Maude *et al.*, Phys. Rev. Lett. **59**, 815 (1990).

[8]J. A. Adams, R. P. Taylor, M. Davies, P. A. Marshall, J. Beerens, S. Charboneau, A. S. Sachrajda, and P. T. Coleridge (unpublished).

[9]P. T. Coleridge, R. P. Taylor, A. S. Sachrajda, and J. A. Adams (unpublished).

[10]R. Landauer, IBM J. Res. Dev. **1**, 223 (1957); M. Buttiker, Phys. Rev. Lett. **57**, 1761 (1986).

[11]C. W. J. Beenakker and H. van Houten, Phys. Rev. B **39**, 10 445 (1989).

[12]P. T. Coleridge, R. P. Taylor, A. S. Sachrajda, and J. A. Adams, Surf. Sci. **305**, 448 (1994).

[13]R. J. Haug, J. Kukera, P. Streda, and K. von Klitzing, Phys. Rev. B **39**, 10 892 (1989).

[14]L. W. Molenkamp *et al.*, Phys. Rev. B **41**, 1274 (1990).

[15]D. A. Wharam, M. Pepper, H. Ahmed, J. E. F. Frost, D. G. Hasko, D. C. Peacock, D. A. Ritchie, and G. A. C. Jones, J. Phys. C **21**, L887 (1988).

[16]R. P. Taylor, A. S. Sachrajda, J. A. Adams, P. T. Coleridge, and P. Zawadski, Physica B **175**, 243 (1991); Superlatt. Microstruct. **11**, 219 (1992).

[17]K. K. Choi, D. C. Tsui, and K. Alavi, Phys. Rev. B **367**, 7751 (1987); R. C. Dynes, Physica B **109**, 1857 (1982). For the electron phase-breaking mechanism, $p=1$ and $\frac{2}{3}$ are predicted for electron-electron momentum-nonconserving scattering processes for two- and one-dimensional systems, respectively. The dimensionality crossover, $L=\pi(\hbar D/kT)^{1/2}$ (where D is the diffusion coefficient), is calculated to occur at $T=4.1$ K for our cavity (note that $\hbar/k\tau=800$ mK).

[18]G. Bergmann, Phys. Rep. **107**, 1 (1984).

[19]G. P. Morris and L. Rondoni (private communication).

[20]A. A. M. Staring, L. Molenkamp. C. W. J. Beenakker, L. Kouvenhoven, and C. T. Foxon, Phys. Rev. B **41**, 8461 (1990). Note that the negative magnetoresistance observed in this work may originate from the Ohmic contacts since a two-terminal measurement was used.

[21]P. C. Main, B. R. Davison, P. H. Beton, L. Eaves, J. R. Owers-Bradley, A. J. M. Neves, S. P. Beaumont, and C. D. W. Wilkinson, J. Phys. Condens. Matter **2**, 6541 (1990).

[22]R. P. Taylor, A. S. Sachrajda, J. A. Adams, P. T. Coleridge, and P. Zawadski, Phys. Rev. B **47**, 4458 (1993).

[23]As in all mesoscopic systems, the mesoscopic potential profile changes when a sample is warmed to 300 K and recooled, due to a repopulation of electron traps; each cooldown effectively yields an additional sample.